Improvement of kesterite solar cell performance by solution synthesized MoO3 interfacial layer

Peer-reviewed author version

Ranjbar, Samaneh; BRAMMERTZ, Guy; Vermang, Bart; Hadipour, Afshin; Cong, Shuren; Suganuma, Katsuaki; Schnabel, Thomas; MEURIS, Marc; da Cunha, A. F. & POORTMANS, Jef (2017) Improvement of kesterite solar cell performance by solution synthesized MoO3 interfacial layer. In: PHYSICA STATUS SOLIDI A-APPLICATIONS AND MATERIALS SCIENCE, 214(1), p. 1-6 (Art N° 1600534).

DOI: 10.1002/pssa.201600534
Handle: http://hdl.handle.net/1942/24107

pss-Header will be provided by the publisher

Improvement of kesterite solar cell performance by solution synthesized MoO_3 interfacial layer

Samaneh Ranjbar[1,4,5*] , Guy Brammertz[2,3], Bart Vermang[2,4,5], Afshin Hadipour[4], Shuren Cong[4,6,7], Thomas Schnabel[8], Marc Meuris[2,3], A. F. da Cunha[1] and Jef Poortmans[3,4,5]

[1] I3N - Departamento de Física, Universidade de Aveiro, Campus Universitário de Santiago, 3810-193 Aveiro, Portugal.
[2] imec division IMOMEC - partner in Solliance, Wetenschapspark 1, 3590 Diepenbeek, Belgium
[3] Institute for Material Research (IMO) Hasselt University, Wetenschapspark 1, 3590 Diepenbeek, Belgium
[4] imec- partner in Solliance, Kapeldreef 75, 3001 Leuven, Belgium
[5] Department of Electrical Engineering (ESAT), KU Leuven, Kasteelpark Arenberg 10, 3001 Heverlee, Belgium
[6] Department of Adaptive Machine Systems, Graduate School of Engineering, Osaka University, 8-1 Mihogaoka, Ibaraki, Osaka 567-0047, Japan.
[7] Infrared Detector Center, Kunming Institute of Physics, 31 Jiaochangdong Road, Kunming, 650223, China
[8] Zentrum für Sonnenenergie- und Wasserstoff-Forschung (ZSW), Industriestraße 6,
70565 Stuttgart, Germany

Received ZZZ, revised ZZZ, accepted ZZZ
Published online ZZZ (Dates will be provided by the publisher.)

Keywords Kesterite $Cu_2ZnSnSe_4$ solar cell, solution synthesized MoO_3, rear contact, open circuit voltage, interface passivation.

In this study an ultra-thin MoO_3 layer synthesized by a solution based technique is introduced as a promising interfacial layer to improve the performance of kesterite $Cu_2ZnSnSe_4$ (CZTSe) solar cell. Solar cells with 10 nm of MoO_3 between Mo rear contact and CZTSe had larger minority carrier life time and open circuit voltage compared to the reference solar cells. Temperature dependent current density-voltage measurement indicated that the activation energy (E_A) of the main recombination is higher (~ 837 meV) in solar cells with MoO_3 layer, as compared to conventional solar cells where E_A ~ 770 meV, indicating reduced interface recombination. A best efficiency of 7.1 % was achieved for a SLG/Mo/MoO_3/CZTSe/CdS/TCO solar cell compared to the reference solar cell SLG/Mo/CZTSe/CdS/TCO for which 5.9 % efficiency was achieved.

1 Introduction Kesterite compounds including $Cu_2ZnSn(S_x,Se_{1-x})_4$ (CZTSSe) [1–4], $Cu_2Zn(Sn_y,Ge_{1-y})(S_x,Se_{1-x})_4$ [5,6], $(Cu_z,Ag_{1-z})_2ZnSn(S_x,Se_{1-x})_4$ [7] are considered as promising candidates for earth abundant thin film photovoltaic technology. However so far device performance of kesterite solar cells is limited to around 12 % that is still far away from the commercial level. One of the main flaws of kesterite solar cell is its low open circuit voltage (V_{oc}), thus a large V_{oc} deficit from the bandgap ($E_g/q-V_{oc}$). Many theoretical and experimental studies have been dedicated to understand the main reasons of large V_{oc} deficit and reduce it. These efforts can be categorized to three main approaches: (1) Improving the absorber layer to reduce the bulk recombination via the tail states and potential fluctuations in the bands. High density of charged defects [8,9], Cu-Zn disorders [10], secondary phases [11,12], grain boundaries [13], etc are counted as the possible reasons of the tail states in kesterite compounds. (2) Improving the band alignment at the p-n junction mainly in Cu_2ZnSnS_4 (CZTS) solar cell in which a cliff-like conduction band offset exists at the CZTS/CdS interface [14,15]. (3) Improving the rear contact by introducing an interfacial layer such as TiN [16–18], TiB [19], Ag [20], ZnO [21,22], Al_2O_3 [23], MoO_2 [24], etc., between Mo and absorber layer. Mo coated glass usually is used as the rear contact in CIGS and kesterite solar cells because of several advantages such as high reflectivity, good resistivity to the corrosive and high temperature selenization/sulfurization process and providing sources for beneficial alkali elements such as Na and K. Despite these advantages two main problems are attributed to the Mo rear contact in kesterite solar cells: (i) The decomposition reactions due to the instability of the Mo/kesterite interface that leads to the formation of secondary phases and voids at the rear surface that affect the film growth, and introduces defects into the absorber layer [16,25]. (ii) The existence of a Schottky barrier at the Mo/ kesterite interface suppresses the

* Corresponding author; e-mail samaneh.ranjbar@ua.pt, Phone: +32 16287726

hole transport and increases the recombination at the rear interface. Based on the thermal behavior of the series resistance (R_s) a barrier height up to 135 meV for CZTSe solar cells [17] and 320 meV for CZTS solar cells [26] are reported. In CIGS solar cell it has been shown that formation of a Mo chalcogenide layer decreases this Schottky barrier height [27]. However in kesterite solar cells the formation of a too thick Mo chalcogenide layer due to the uncontrolled reaction between Mo and kesterite can be detrimental to the solar cell performance [18,25]. To address these issues related to the Mo rear contact, different interfacial layers have been introduced between the Mo and absorber layer. TiN layer was reported as a promising candidate to avoid the decomposition reactions [16] and also to improve the band alignment by decreasing the barrier height to 15 meV [17]. Ultra-thin ZnO layer was also introduced as an inert layer for avoiding the decomposition reactions [21,22], although it's an n-type semiconductor and it can alter the band alignment. Recently, using thermally evaporated MoO_2 layer, large open circuit voltage (V_{oc}) around 460 meV was achieved for a CZTSe solar cell [24]. We tried sputtered TiN and ZnO as interfacial layers, but no improvement has been achieved compared to our base line solar cells. Here we will introduce a MoO_3 interfacial layer synthesized by an easy, fast and very reproducible solution based process. Solution processed MoO_3 is an appropriate interfacial layer for the rear contact application because it is a wide band gap p-type semiconductor (~ 3.8 eV) with high work function (~ 6.8 eV [28]) compared to the Mo rear contact that has a work function around 4.5 eV. Using a solution-based method has many advantages compared to thermally evaporated MoO_{3-x} layer. Besides reproducibility, feasibility, cost effectivity and industrial viability, solution-based techniques lead to conservation of highest oxidation state 6+ for the MoO_3 layer, hence keeping its work function as high as possible. When MoO_3 material is thermally evaporated - due to heat - some amount of oxygen is lost during the processing, which leads to lowering the oxidation state of it and formation of MoO_{3-x} $_{(0<x<1)}$ layer. Lower oxidation states of MoO_{3-x} leads to lower work function (MoO_2 work function is ~ 5.9 eV [28]) compared to high work function of MoO_3. The Schottky barrier (ϕ_b) at the interface of a metal/ p-type semiconductor depends on the work function of the metal, the bandgap (E_g) and electron affinity (χ) of the semiconductor [29]:

$$\phi_b = E_g + \chi - \phi_m \quad (1)$$

Therefore by using p-type interfacial layer with high work function the barrier height will decrease and disappear if $\phi_m \geq (E_g + \chi)$. According to our previous study, the thickness of the absorber layer is an important factor for the performance of CZTSe solar cells. We observed that by increasing the thickness of the absorber layer the performance of the solar cells improved significantly and part of this improvement was attributed to less recombination at the rear interface. By increasing the thickness, the distance between the p-n junction and the rear surface decreases which leads to less rear interface recombination and enhancement of the minority carrier life time and V_{oc} [30]. thus in this study we aim to introduce an appropriate interfacial layer at the rear interface of kesterite solar cell, mainly to improve the band alignment, avoid the decomposition reactions and enhance the rear interface quality.

2 Experimental Two types of rear contact were used in this study: (i) conventional Mo coated Soda Lime Glass, SLG/Mo and (ii) Mo coated SLG with an ultra-thin layer of MoO_3 (thickness ~ 10 nm), SLG/Mo/MoO_3. MoO_3 was synthesized by spin coating of Ammonium Molybdate on SLG/Mo substrate and then annealing on a hot plate at 200 ºC for 10 min. More details about synthesizes and physical characterization of MoO_3 layer were explained in Ref. [31]. CZTSe absorber layers were prepared in a two-stage process. In the first stage Sn, Zn and Cu were subsequently deposited on the rear contact by e-beam evaporation. The Sn/Zn/Cu stacks were then selenized by 10 % H_2Se gas diluted in N_2 for 15 min at 460 °C in a rapid thermal processing system with 1 °C/s heating rate. Here the effect of the MoO_3 interfacial layer for two types of solar cells is investigated: (a) solar cells with thin absorber layers prepared by selenization of Sn(215 nm)/Zn(100 nm)/Cu(110 nm) stack and (b) solar cells with thick absorber layers prepared by selenization of Sn(310 nm)/Zn(150 nm)/Cu(160 nm) stack. The final thickness of the absorber layers after the selenization is measured by cross sectional scanning electron microscopy (SEM) to be around 1 µm and 1.7 µm for the thin and thick absorbers, respectively. Solar cells were then synthesized after KCN treatment, chemical bath deposition of CdS (~ 50 nm), sputtering of intrinsic ZnO (~ 50 nm) and Al-doped ZnO (~ 300-400 nm) and finally evaporation of Ni/Al/Ni grids. Solar cells with 0.5 cm^2 area were isolated laterally by needle scribing. Solar cells were annealed in N_2 atmosphere at 200 ºC for 1 hour and all the optical and electrical characterizations reported here are performed after the post annealing step. The beneficial impact of this post annealing step was already reported by several groups [32]. Samples are named according to their rear contact type: with MoO_3 layer (S) and without MoO_3 layer (R). S/R-(i=1,2) samples are made from thin absorber layer while S/R-(i=3,4) are made from thick absorber layer. Room temperature Time Resolved-Photoluminescence (TR-PL) measurements were acquired by a Hamamatsu C12132. An area of 3 mm diameter of solar cells was illuminated by a 532 nm laser with 15 kHz repetition rate and 1.0 mW average power. Current density -Voltage (J-V) measurements of solar cells were performed using a Wacom solar simulator under standard AM1.5 spectrum and 1 sun illumination.

Table 1. Electrical parameters of the best solar cells of the samples with different rear contact and absorber thickness: short circuit current (J_{sc}), open circuit voltage (V_{oc}), fill factor (FF), efficiency (η), shunt resistance (R_{sh}), series resistance (R_s) and ideality factor (A) are derived from illuminated current-voltage (J-V) measurement.

Sample	Rear contact	Thick-ness (μm)	V_{oc} (mV)	J_{sc} (mA.cm2)	FF (%)	η (%)	R_{sh} ($\Omega.cm^2$)	R_s ($\Omega.cm^2$)	A (/)
R-1	Mo	1	395	23.9	43.2	4.1	113	1.3	3.1
S-1	Mo/MoO_3	1	441	24.7	36.8	4	171	1	3.9
R-4	Mo	1.7	384	32.8	47	5.9	164	2.1	2.6
S-4	Mo/MoO_3	1.7	413	32.9	52.3	7.1	311	1.7	2.4

Compositional depth profiles of elements are recorded by glow discharge optical emission spectroscopy (GDOES) using a Horiba Scientific GD-Profiler 2 operated in RF-mode at powers of 26 W and argon pressures of 5 mbar. The measurement spot has a diameter of 4 mm and a depth-resolution within the absorber of about 60 nm is achieved. The morphology and the composition of the films were investigated by scanning electron microscopy (SEM) and energy dispersive spectrometry (EDS), using a TESCAN Vega 3 SBH equipped with a Bruker EDS system.

3 Results and discussions In Fig.1 (a) and (b) the TR-PL spectra of the solar cells with Mo and Mo/MoO_3 rear contacts are compared for thin and thick devices, respectively. The PL decay curves are fitted to a two exponential function and the slower decay time (τ) is considered to be correlated to the minority carrier lifetime. Solar cells with MoO_3 layer have longer PL decay time compared to the reference samples. Generally the PL decay time is also remarkably longer for thicker devices, thus it can be concluded that both the rear surface and the bulk quality of CZTSe solar cells affect the recombination and consequently the minority carrier lifetime. The photoluminescence spectra of the thin and thick solar cells are also shown in Fig.1 (c) and (d), respectively. It can be observed that the PL peaks of solar cells with MoO_3 layer move slightly toward higher energies closer to the band gap of CZTSe (1 eV). The PL peak shift is more pronounced in thin solar cells in which the effect of rear surface is more sensible. It is reported that the PL peak position of kesterite solar cells is lower than their bandgap due to the existence of large amount of tail states and potential fluctuation [8,33]. Part of the tail states in kesterite can be attributed to the formation of defects such as Sn and Se vacancies due to the decomposition reactions at the rear surface [25].

In Fig.2 the device parameters of 4 samples (each sample includes at least 12 solar cells) with MoO_3 layer (S-i=1-4) are compared with their references (R-i=1-4) (e.g. S-1 is prepared under the same condition as its reference R-1). In general, by introducing the MoO_3 layer the V_{oc} improved significantly while short circuit current (J_{sc}) and Fill Factor (FF) did not change considerably. Moreover, J_{sc} and FF improved significantly by increasing the thickness, mainly due to an enhanced bulk quality of the CZTSe absorber layer - as described in our previous study [30]. The AM 1.5 illuminated Current density-Voltage (J-V) curve of the champion solar cells with/without the MoO_3 layer of one of the thin samples (S/R-1) and one of the thick samples (S/R-4) are illustrated in Fig.3 (a) and (b), respectively. The diode parameters of the devices are derived by the procedure explained in Ref. [34], and are summarized in Table.1.

Figure 1 Room temperature TR-PL spectra of the samples with and without MoO_3 layer (a) thin samples and (b) thick samples. Room temperature PL spectra of thin (c) and thick samples (d).

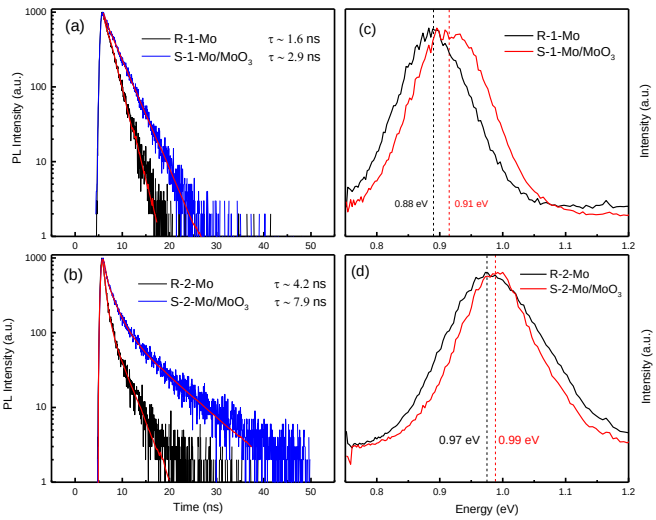

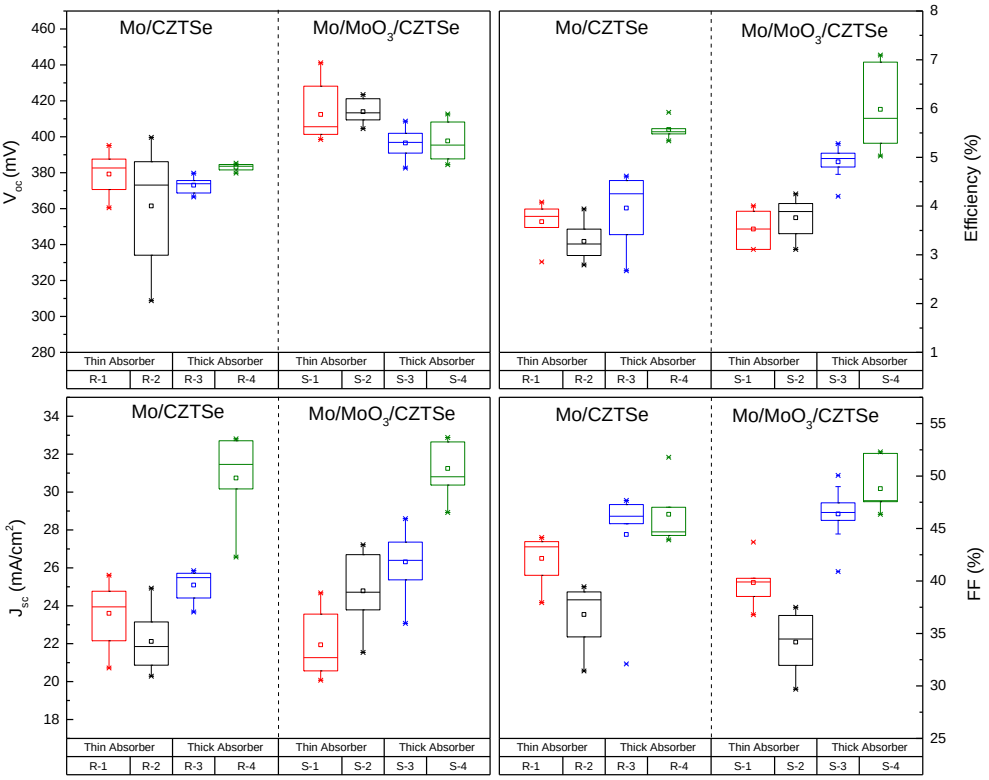

Figure 2 Electrical parameters of the samples made with/without MoO_3 layer (S/R). Each box represents values measured from samples containing at least 12 solar cells.

Introducing the MoO_3 layer leads to the significant improvement of V_{oc} from 395 to 441 mV for thin solar cells and from 384 to 413 mV for thick solar cells. Even though solar cell S-1 has a relatively large V_{oc} of 441 mV, it is suffering from low FF and quite large ideality factor. Large ideality factor above 2 indicates peculiar recombination mechanisms such as tunneling enhanced recombination, donor-acceptor pair recombination or fluctuation of activation energy of the main recombination path [35]. The illuminated and dark J-V curve of the best thin solar cells R-1 (without MoO_3) and S-1 (with MoO_3) were measured at different temperatures. Thermal behavior of V_{oc}, series resistance, Arrhenius plot of series resistance and ideality factor/dark saturation current are illustrated in Fig.3 (c), (d), (e), (f), respectively. As can be seen in Fig.3 (c) solar cells with and without MoO_3 layer show quite similar series resistance (R_s) thermal behavior. By making an Arrhenius plot of R_s the barrier height (ϕ_b) is estimated [34] to be
around 30 meV for both solar cells, i.e. with and without MoO_3 layer (See Fig.3 (d)). Low barrier height of S-1 and R-1 indicates a good band alignment between Mo and CZTSe and can be due to the formation of a thin $MoSe_2$
layer ($MoSe_2$ is found in the XRD pattern of the solar cells, not shown). In Fig.3 (e) the thermal behavior of the solar cells S-1 and R-1 are shown. The temperature dependence of V_{oc} can be explained by Eq. (2):

$$V_{oc} = \frac{E_A}{q} - \frac{AkT}{q} \ln\left(\frac{J_{00}}{J_L}\right) \quad (2)$$

where E_A, A, k, J_{00}, and J_L are the activation energy, diode ideality factor, Boltzmann constant, reverse saturation current pre-factor, and the photocurrent, respectively [34]. Reverse saturation current pre-factor is related to the dark saturation current according to Eq. (3):

$$J_0 = J_{00} \exp(-\frac{E_A}{AkT}) \quad (3)$$

Generally, the activation energy (E_A) is correlated to the main recombination path in the solar cell. When the bulk recombination is dominant then $E_A \sim E_g/q$ (E_g is the band gap of the absorber layer) while in case of interface recombination (including the rear or front interface) $E_A < E_g/q$ [34,35]. However, other factors such as band gap fluctuation in the absorber layer (that is also very likely in CZTSe) can also lead to lower activation energy than bandgap [35]. As shown in Fig.3 (e), a solar cell with MoO_3 has higher E_A around 837 meV compared to the reference solar cell for which E_A is around 770 meV. Higher activation energy of solar cells with MoO_3 interfacial layer along with other results including longer minority carrier life time and larger V_{oc} indicate the suppression of rear interface recombination.

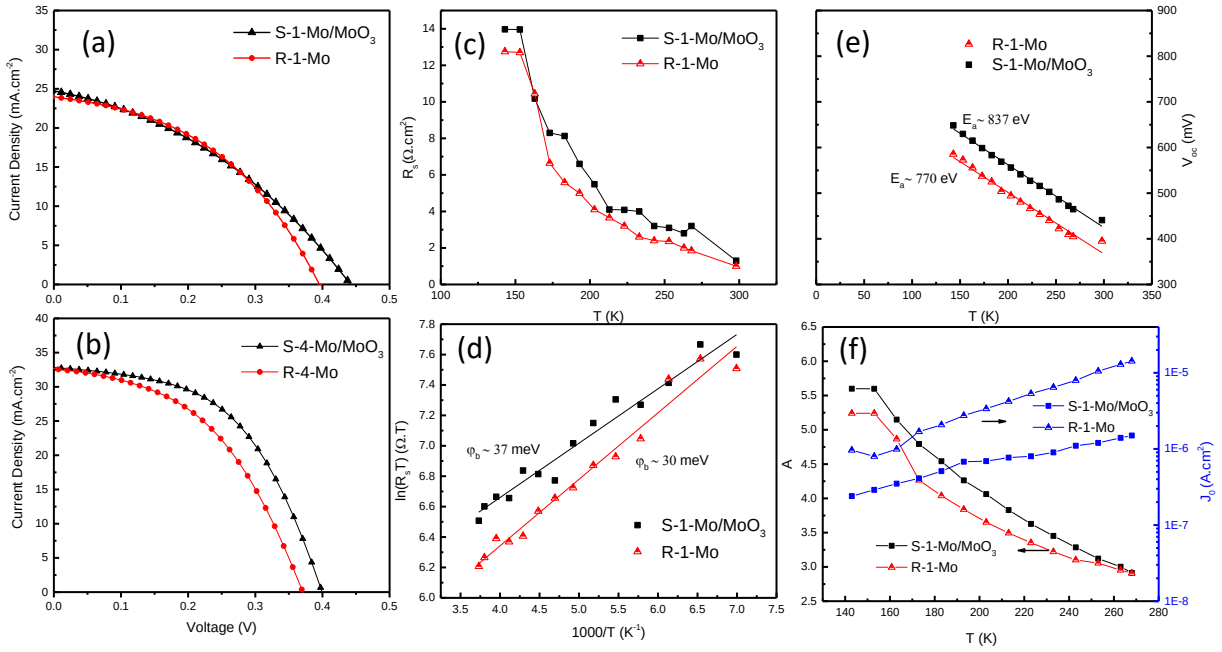

Figure 3 (a) AM 1.5 illuminated J-V curve of the champion solar cells with/without the MoO_3 layer of one of the thin samples (S/R-1) and (b) one of the thick samples (S/R-4). (c) Thermal behavior of series resistance (R_s), (d) Arrhenius plot of R_s, (e) Thermal behavior of V_{oc} and (f) ideality factor (A)/dark saturation current (J_0) of the best thin solar cells with/without MoO_3 layer (S-1/R-1).

Several studies have already mentioned the instability of Mo during the selenization/sulfurization process that leads to the formation of voids, secondary phases and introducing the defects such as Se vacancies [16-25]. Based on the optical and electrical measurements of this study, the beneficial effects of MoO_3 layer is mainly due to the suppression of rear interface recombination. This might be due to the reduction of the decomposition reactions at the rear interface and improving the rear surface quality with less voids, secondary phases and defects. Another hypothesis could be the role of oxygen in passivation of defects, as in high temperature processing the oxygen can be released and fill the different vacancies.

Ideality factor and dark saturation current of the solar cells with and without MoO_3 layer at various temperature derived at intermediate bias voltage (0.2-0.3 V), are shown in Fig.3 (d). Solar cells show strong ideality factor temperature dependent behavior that might be explained by enhanced tunneling recombination [35,36].

In order to investigate the impact of the MoO_3 layer on the diffusion of alkali element such as Na, GDOES measurement were performed on solar cells after removing the transparent conducting oxide and CdS layers by etching in diluted HCl. In Fig.4 (a) and (b) the depth profile of different elements including Na in the reference solar cell R-4 (with Mo rear contact) and S-4 (with Mo/MoO_3 rear contact) are shown, respectively. Also in the inset top view SEM images of the corresponding absorber layers after removing the top layers are shown. The GDOES measurements indicate that Na diffusion is even slightly higher in solar cells with MoO_3 layer compared to the reference solar cells, thus MoO_3 layer is not a barrier for diffusion of Na.

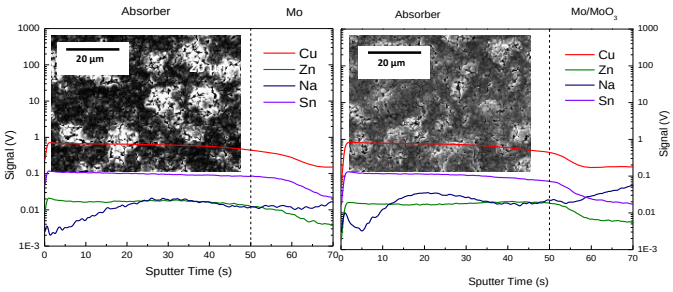

Figure 4 (a) GDOES measurements of SLG/Mo/CZTSe and (b) SLG/Mo/MoO_3/CZTSe. Sputter time = 0 s is the top surface of the CZTSe absorber layer.

SEM images revealed that the absorber layers especially the one prepared on conventional Mo substrate suffer from the existence of too many voids and secondary phases mainly ZnSe. The average chemical composition of normal regions (such as A in the inset of Fig.4 (a)) measured with EDS was Zn/Sn ~ 1.1, Cu/(Zn+Sn) ~ 0.8, and Se/(Cu+Zn+Sn) ~ 1.1. While, the average composition of the white spots (B) was Zn/Sn ~ 4, Cu/ (Zn+Sn) ~ 0.3 and Se / (Cu+Zn+Sn) ~ 1.5. The CZTSe layer prepared on Mo/MoO_3 substrate looks more compact and uniform with less secondary phases compared to the CZTSe layer on Mo substrate. Better morphology can be achieved due to the improvement of rear surface quality and better growth condition.

5 Conclusions In this study the effect of rear contact on the performance of two types of CZTSe solar cells including solar cells with thin and thick absorber layer was studied. It was shown that by introducing an ultra-thin layer of MoO_3 between Mo rear contact and CZTSe absorber layer the minority carrier life time and V_{oc} improve remarkably for both of the thin and thick solar cells. J_{sc} and FF did not change considerably by introducing the MoO_3 layer but they improved significantly by increasing the absorber layer thickness. The temperature dependent J-V measurement showed that the band alignment at the rear interface doesn't change considerably by adding the MoO_3 layer and the activation energy of the main recombination path shifts toward the higher energies. Top view SEM images of the absorber layers revealed that samples prepared on MoO_3 layer are more uniform and compact. Thus, according to these measurements, the main role of MoO_3 layer can be explained as avoiding or reducing of the reaction between Mo and CZTSe during the selenization process that leads to less voids and secondary phases at the rear surface and passivation of defects. The best solar cell in this study was the thick one with MoO_3 interfacial layer that has 7.1 % conversion efficiency.

Acknowledgements This project has received funding from the European Union's Horizon 2020 research and innovation program under grant agreement No 640868. This research is partially funded by the Flemish government, Department Economy, Science and innovation. This work is also funded by FEDER funds through the COMPETE 2020 Programme and National Funds through FCT - Portuguese Foundation for Science and Technology under the project UID/CTM/50025/2013. S. Ranjbar acknowledges the financial support of the Portuguese Science and Technology Foundation (FCT) through PhD grant SFRH/BD/78409/2011. B. Vermang acknowledges the financial support of the Flemish Research Foundation FWO (mandate 12O4215N).

References

[1] H. Katagiri, K. Jimbo, W.S. Maw, K. Oishi, M. Yamazaki, H. Araki and A. Takeuchi, Thin Solid Films. **517,** 2455 (2009).

[2] G. Brammertz, M. Buffière , S. Oueslati, H. Elanzeery, K. Ben Messaoud, S. Sahayaraj, C. Köble, M. Meuris and J. Poortmans, Appl. Phys. Lett. **103**, 163904 (2013).

[3] P.A. Fernandes, P.M.P. Salomé, A.F. Cunha, B. Schubert, Thin Solid Films. **519**, 7382 (2010).

[4] W. Wang, M.T. Winkler, O. Gunawan, T. Gokmen, T.K. Todorov, Y. Zhu and D.B. Mitzi, Adv. Energy Mater. **4**, 1 (2014).

[5] A.D. Collord and H.W. Hillhouse, Chem. Mater. **28**, 2067 (2016).

[6] M. Neuschitzer, J. Marquez, S. Giraldo, M. Dimitrievska, M. Placidi, I. Forbes, V. Izquierdo-roca, A. Pérez-Rodriguez and E. Saucedo, J. Phys. Chem. C **120**, 9661, (2016).

[7] T. Gershon, Y.S. Lee, P. Antunez, R. Mankad, S. Singh, D. Bishop, O. Gunawan, M. Hopstaken and R. Haight, Adv. Energy Mater. **6**, 1502468 (2016).

[8] T. Gokmen, O. Gunawan, T.K. Todorov, D.B. Mitzi, T. Gokmen, O. Gunawan, T.K. Todorov and D.B. Mitzi, **103506**, 11 (2016).

[9] BG Mendis, MD Shannon, MCJ Goodman, JD Major, AA Taylor, DP Halliday and K Durose, J. Phys. Conf. Ser., **471,** 012014 (2013).

[10] J.J. Scragg, Jes K. Larsen, M. Kumar, C. Persson, J. Sendler, S. Siebentritt and Charlotte Platzer Björkman, Phys. Status Solidi B, **253**, 247 (2015).

[11] G. Altamura and J. Vidal, Chem. Mater. **28**, 3540 (2016).

[12] J. Just, D. Lützenkirchen-Hecht, R. Frahm, S. Schorr and T. Unold , Appl. Phys. Lett. **99**, 262105 (2011).

[13] W. Yin, Y. Wu, S. Wei, R. Noufi, M.M. Al-jassim, Adv. Energy Mater. **4**, 1300712, (2014)

[14] F. Liu, C. Yan, J. Huang, K. Sun, F. Zhou, J.A. Stride, M.A. Green, X. Hao, Adv. Energy Mater. (2016), 1600706. doi:10.1002/aenm.201600706

[15] C. Platzer-Björkman, C. Frisk, J.K. Larsen, T. Ericson, S. Li, J.J.S. Scragg, J. Keller, F. Larsson and T. Törndahl, Appl. Phys. Lett. **107**, 243904 (2015).

[16] J.J. Scragg, T. Kubart, J.T. Watjen, T. Ericson, M.K. Linnarsson, C. Platzer-Björkman, Chem. Mater. **25**, 3162 (2013).

[17] S. Oueslati, G. Brammertz, M. Buffière, H. ElAnzeery, D. Mangin, O. ElDaif, O. Touayar, C. Köble, M. Meuris, J. Poortmans, J. Phys. D. Appl. Phys. **48**, 035103 (2015).

[18] B. Shin, Y. Zhu, N.A. Bojarczuk, S.J. Chey, S. Guha, B. Shin, Y. Zhu, N.A. Bojarczuk, S.J. Chey, S. Guha, Appl. Phys. Lett. **102**, 091907 (2013)

[19] F. Liu, K. Sun, W. Li, C. Yan, H. Cui, L. Jiang, X. Hao, A. Martin, Appl. Phys. Lett. **104**, 051105 (2014).

[20] H. Cui, X. Liu, F. Liu, X. Hao, N. Song, C. Yan, H. Cui, X. Liu, F. Liu, X. Hao, N. Song, C. Yan, Appl. Phys. Lett. **104**, 041115 (2014).

[21] S. López-Marino, M. Placidi, A. Pérez-Tomás, J. Llobet, V. Izquierdo-Roca, X. Fontané, A. Fairbrother, M. Espíndola-Rodríguez, D. Sylla, A. Pérez-Rodríguez and E. Saucedo, J. Mater. Chem. A. **1,** 8338, (2013).

[22] W. Li, J. Chen, H. Cui, F. Liu, X. Hao, Materials Letters, **130**, 87 (2014).

[23] B. Vermang, Y. Ren, O. Donzel-Gargand, C. Frisk, J. Joel, P. Salome, J. Borme, S. Sadewasser, C. Platzer-Bjorkman and M. Edoff, IEEE J. Photovoltaics. **6**, 332 (2015).
[24] S. López-marino, M. Espíndola-Rodríguez, Y. Sánchez, X. Alcobé, F. Olivaa, H. Xie, M. Neuschitzer, S. Giraldo, M. Placidi, R. Caballero, V. Izquierdo-Roca, A. Pérez-Rodríguez and E. Saucedo, Nano Energy **26**, 708 (2016).
[25] J.J. Scragg, J.T. Watjen, M. Edoff, T. Ericson, T. Kubart, C. Platzer- Björkman, , J. Am. Chem. Soc. **134,** 19330 (2012).
[26] K. Wang, O. Gunawan, T. Todorov, B. Shin, S.J. Chey, N.A. Bojarczuk, D. Mitzi, S. Guha, , Appl. Phys. Lett. **97**, 2 (2010).
[27] K.-J. Hsiao, J.-D. Liu, H.-H. Hsieh, T.-S. Jiang, Phys. Chem. Chem. Phys. **15**, 18174 (2013).
[28] M.T. Greiner, Z. Lu,, NPG Asia Mater. **5**, e55, (2013)
[29] S. Adachi, Earth-Abundant Materials for Solar Cells: Cu_2-II-IV-VI_4 Semiconductors, (John Wiley & Sons, Japan, 2015), p 235.
[30] S. Ranjbar, G. Brammertz, B. Vermang, A. Hadipour ,M. Sylvester, A. Mule, M. Meuris, A.F. da Cunha and J. Poortmans, On the effect of absorber thickness in kesterite thin film solar cells, Thin Solid Films, to be published.
[31] K.S. Shuren Cong, Tohru Sugahara, Tingting Wei, Jinting Jiu, Yukiko Hirose, Shijo Nagao, No Title, Cryst. Growth Des. **15**, 4536 (2015).
[32] D. Hironiwa, N. Sakai, T. Kato, H. Sugimoto, Z. Tang, Thin Solid Films. **582**, 151 (2015).
[33] S. Oueslati, G. Brammertz, M. Buffière, C. Köble, T. Oualid, M. Meuris, J. Poortmans, Sol. Energy Mater. Sol. Cells. **134**, 340 (2015).
[34] S.S. Hegedus, W.N. Shafarman, Prog. Photovoltaics Res. Appl. **12**, 155 (2004).
[35] R. Scheer and H. W. Schock, Chalcogenide Photovoltaics (Wiley-VCH, Weinheim, Germany, 2011).
[36] U. Rau, H.W. Schock, Appl. Phys. A **69**, 131 (1999).